Journal of Medicinal Chemistry

Article

Identification of Novel Extracellular Signal-Regulated Kinase Docking Domain Inhibitors

Chad N. Hancock, Alba Macias, Eun Kyoung Lee, Su Yeon Yu, Alexander D. MacKerell,, and Paul Shapiro

J. Med. Chem., **2005**, 48 (14), 4586-4595• DOI: 10.1021/jm0501174 • Publication Date (Web): 21 June 2005

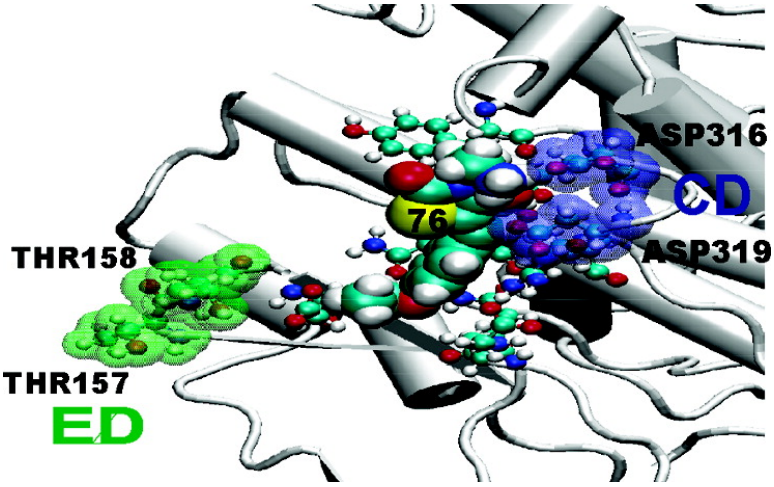

More About This Article

Additional resources and features associated with this article are available within the HTML version:

- Supporting Information
- Links to the 6 articles that cite this article, as of the time of this article download
- Access to high resolution figures
- Links to articles and content related to this article
- Copyright permission to reproduce figures and/or text from this article

View the Full Text HTML

Journal of Medicinal Chemistry is published by the American Chemical Society. 1155 Sixteenth Street N.W., Washington, DC 20036

Identification of Novel Extracellular Signal-Regulated Kinase Docking Domain Inhibitors

Chad N. Hancock,[†] Alba Macias,[‡] Eun Kyoung Lee,[‡] Su Yeon Yu,[‡] Alexander D. MacKerell, Jr.,*[,‡] and Paul Shapiro*[,†,‡]

Department of Pharmaceutical Sciences, School of Pharmacy, and Molecular and Cell Biology Program, University of Maryland, Baltimore, Maryland 21201

Received February 7, 2005

The extracellular signal regulated kinase (ERK1 and ERK2) signal transduction pathways play a critical role in cell proliferation. Hyperactivation of the ERK proteins either through increased expression of membrane-bound growth factor receptors or genetic mutations of upstream proteins is thought to be involved in the pathogenesis of many human cancers. Thus, targeted inhibition of ERK signaling is viewed as a potential approach to prevent cancer cell proliferation. Currently, no specific inhibitors of the ERK proteins exist. Moreover, most kinase inhibitors lack specificity because they target the ATP binding region, which is well conserved among the protein kinase families. Taking advantage of recently identified ERK docking domains, which are reported to facilitate substrate protein interactions, we have used computer-aided drug design (CADD) to identify novel small molecular weight ERK inhibitors. Following a CADD screen of over 800 000 molecules, 80 potential compounds were selected and tested for activity in biological assays. Several compounds inhibited ERK-specific phosphorylation of ribosomal S6 kinase-1 (Rsk-1) or the ternary complex factor Elk-1 (TCF/Elk-1), both of which are involved in promoting cell proliferation. Active compounds showed a dose-dependent reduction in the proliferation of several cancer cell lines as measured by colony survival assays. Direct binding between the active compounds and ERK2 was indicated by fluorescence quenching. These active compounds may serve as lead candidates for development of novel specific inhibitors of ERK−substrate interactions involved in cell proliferation.

Introduction

Mitogen-activated protein (MAP) kinases consist primarily of the extracellular signal-regulated kinases 1 and 2 (ERK1/2), c-Jun N-terminal kinases (JNK), and p38 MAP kinases.[1] MAP kinases play a central role in the regulation of most biological processes including cell growth, proliferation, differentiation, inflammatory responses, and programmed cell death. Unregulated activation of MAP kinases has been linked to cancer cell proliferation and tissue inflammation.[2−5] Thus, the development of specific MAP kinase inhibitors is viewed as an effective approach toward the identification of novel chemotherapy and antiinflammatory agents.[6]

Activation of ERK proteins most often occurs through a process where a ligand-activated plasma membrane receptor facilitates the sequential activation of the Ras G-proteins, Raf kinases, and the MAP or ERK kinases-1 and -2 (MEK1/2), which are the only known activators of ERK1 and ERK2.[7] The activation of ERK proteins by MEK1/2 is regulated by direct phosphorylation of threonine (Thr) 183 and tyrosine (Tyr) 185 (amino acid numbering according to mouse sequence, accession #P63085), where phosphorylation of both sites is required for full activation. Once ERK is phosphorylated, it undergoes structural changes that are important for phosphoryl transfer onto substrate proteins.[8] In vitro studies suggest that active ERK proteins may phosphorylate more than 50 different substrates.[1,7] However, it is not clear whether all of these substrates are physiological targets in vivo or whether activated ERK selectively phosphorylates specific substrates in response to a particular extracellular signal. Importantly, hyperactivation of the ERK MAP kinases has been linked to unregulated cell proliferation in cancer cells. For example, naturally occurring mutations in Ras and Raf proteins, which cause hyperactivation of the ERK pathway, are found in almost 30% of all human cancers.[3,9,10]

The mechanisms involved in determining the interactions between the ERK proteins and their cognate substrate proteins are still largely unknown. Similarly, it is not clear how ERK distinguishes between its own protein substrates and substrates that are phosphorylated by the JNK or p38 MAP kinases. Studies in recent years have revealed at least three protein motifs that provide clues as to how ERK proteins interact with and phosphorylate specific substrate proteins. First, ERK proteins are proline-directed serine or threonine kinases that prefer the consensus PXS/TP (X is any amino acid, P is proline, S is serine, and T is threonine) motif on the substrate protein.[11] At a minimum, ERK proteins require a proline that is immediately C-terminal to the phosphorylated S or T residue. Second, ERK substrates may contain an FXFP (F is phenylalanine) motif, a D-domain containing basic residues followed by an LXL motif, or a kinase interaction motif (KIM), which are important for substrate interactions with ERK.[12,13]

* To whom correspondence should be addressed. Phone: 410-706-8522 (P.S.), 410-706-7442 (A.M.). Fax: 410-706-0346. E-mail: pshapiro@rx.umaryland.edu or amackere@rx.umaryland.edu.
[†] Molecular and Cell Biology Program.
[‡] Department of Pharmaceutical Sciences, School of Pharmacy.

10.1021/jm0501174 CCC: $30.25
Published on Web 06/21/2005

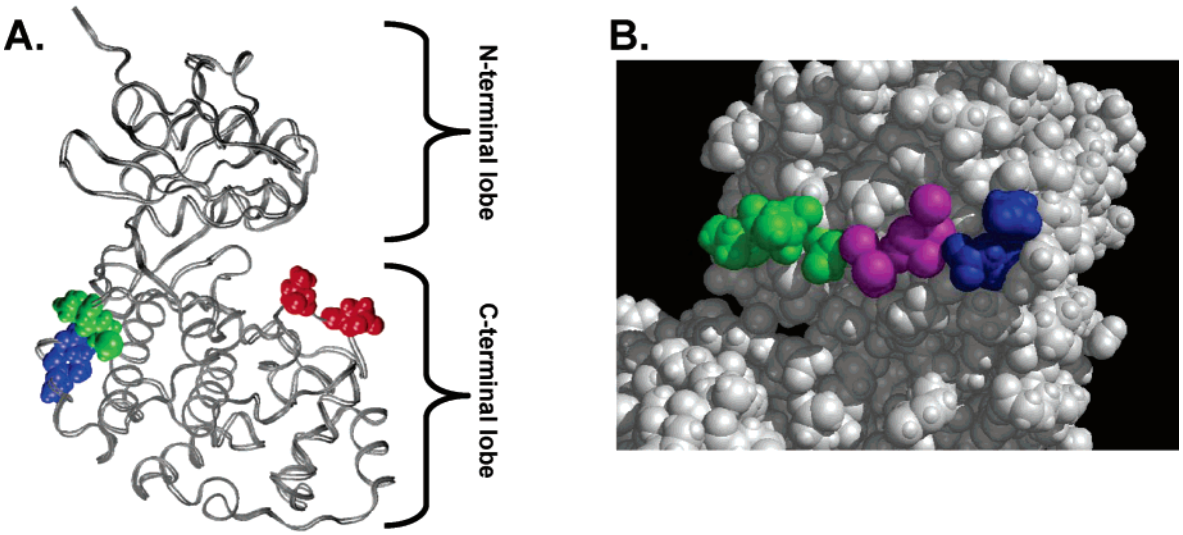

Figure 1. ERK2 structure and location of docking domains. (A) Ribbon diagram of the 3D structure of the unphosphorylated form of ERK2 showing the spatial relationship of the ERK2 phosphorylation sites and the docking region. Phosphorylation residues Thr183 and Tyr185 are red spheres, common docking (CD) residues Asp316 and Asp319 are blue spheres, and the ED residues Thr157 and Thr158 are green spheres. (B) Space filling diagram of putative docking groove located between the CD and ED residues. The unphosphorylated form of ERK2 (white spheres) showing the common docking (CD) residues Asp316 and Asp319 as blue spheres and the ED residues Thr157 and Thr158 as green spheres and the sphere set defining the putative binding pocket of the docking domains as purple spheres.

Third, ERK proteins contain recently identified docking domains that have been shown to facilitate interactions with substrate proteins.[14−16] The first identified ERK2 docking domains, referred to as the common docking (CD) and ED domain, are positioned opposite the activation loop in the 3D crystallographic structure and appear to regulate the efficiency of substrate phosphorylation and interaction with the upstream MEK proteins (Figure 1).[16] More recent data suggest that additional amino acid residues in the C-terminal domain of ERK2 may also form additional docking domains that regulate specific substrate interactions.[14]

No specific inhibitors of the ERK proteins are currently available. Pharmacological inhibitors of Ras G-proteins, Raf kinases, and MEK1/2 have been used successfully to block the ERK pathway and are being tested in cancer clinical trials.[17−20] However, since ERK proteins are involved in many cellular functions, it may be more beneficial to selectively block ERK involvement in abnormal cell functions such as cancer cell proliferation while preserving ERK functions in regulating normal metabolic processes.

Given that most kinase inhibitors lack specificity because they compete with ATP binding domains that are conserved among protein kinases,[6,21] we hypothesized that small molecular weight compounds that interact with specific ERK docking domains can be used to specifically disrupt ERK2 interactions with protein substrates. Taking advantage of the ERK2 crystal structure, we have used computer-aided drug design (CADD)[22] to identify low molecular weight compounds that interact with the CD and ED docking domain region of ERK2. Recent successes in CADD approaches in the identification of inhibitors of protein−protein interactions[23−26] indicated that such an approach was feasible for the present system. In the present study, using CADD screening of a virtual database followed by experimental assays, we have identified several low molecular weight compounds that disrupt ERK function by inhibiting ERK-specific phosphorylation of the Rsk-1 and Elk-1 substrates. Moreover, biological assays revealed that the lead compounds were effective in preventing proliferation of cancer cell lines.

Experimental Section

CADD in Silico Screening. The 3D structure of ERK2 in the unphosphorylated state[27,28] was retrieved from the Protein DataBank.[29] Charges and hydrogens were added using SYBYL6.4 (Tripos, Inc.). All docking calculations were carried out with DOCK[30] using flexible ligands based on the anchored search method.[31] The solvent accessible surface[32] was calculated with the program DMS[33] using a surface density of 2.76 surface points per Å^2 and a probe radius of 1.4 Å^2. Sphere sets were calculated with the DOCK associated program SPHGEN. From the full sphere set, sphere clusters in the ERK2 docking domains important for interactions with the protein substrates were identified. On the basis of mutagenesis experiments, residues involved in intermolecular interactions were used to select the docking site. These include Asp316 and Asp319 in the C-terminus,[16] which are part of the common docking (CD) domain, and residues Thr157 and Thr158, which contribute to the ED docking domain.[34] Spheres within both 10 Å of the CD domain and 12 Å of the ED domains were selected. The resulting sphere set contained 11 spheres and was located in the groove between the CD and ED domains as shown in Figure 1. The selected sphere set acted as the basis for initial ligand placement during database searching. The GRID method[35] within DOCK was used to approximate the ligand−receptor interaction energy during ligand placement by the sum of the electrostatic and van der Waals (vdW) components. The GRID box dimensions were 25.3 × 26.6 × 27.3 Å^3 centered around the sphere set to ensure that docked molecules were within the grid.

A database of more than 800 000 compounds was used for the initial virtual screening. These database of low molecular weight, commercially available compounds had been created in our laboratory by converting files obtained from the vendors in the 2D SDF format to the 3D MOL2 format through a procedure that included geometry generation, addition of hydrogens and charges, and force field optimization using SYBYL6.4 along with in-house programs.[26,36] The compounds that were screened had between 10 and 40 heavy atoms and less than 10 rotatable bonds. During the docking procedure,

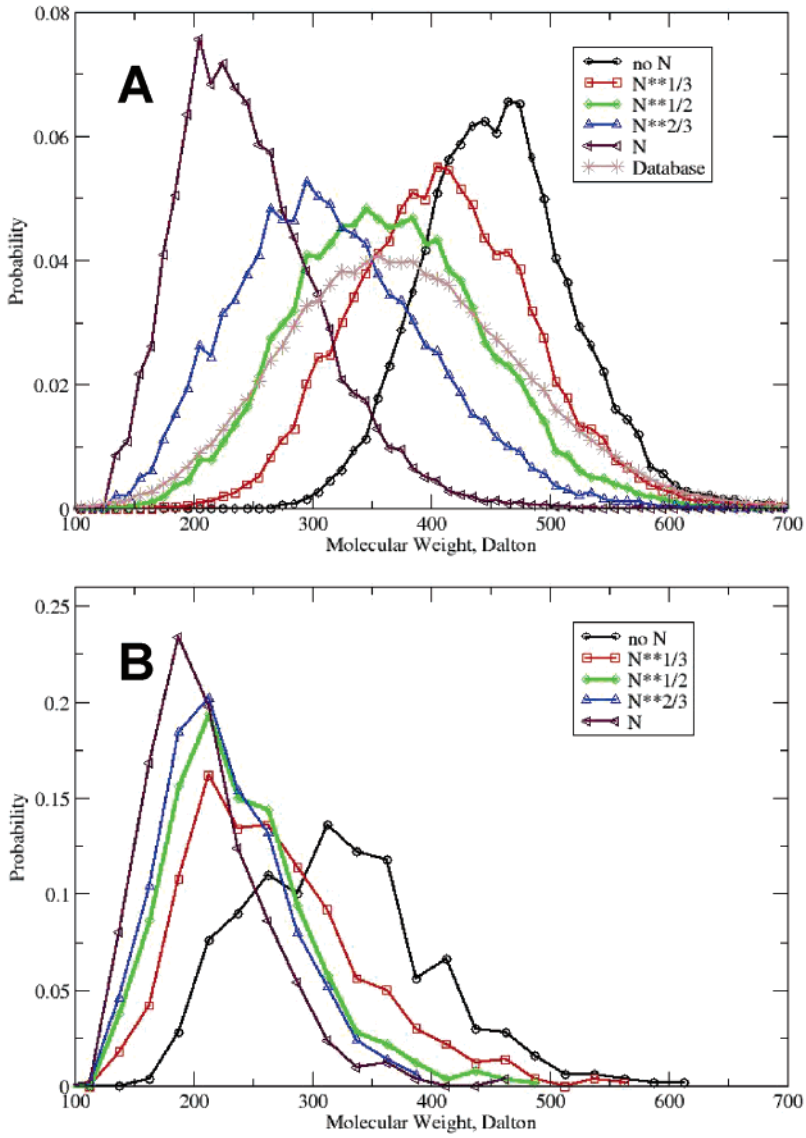

Figure 2. Molecular weight distribution of top compounds. (A) Molecular weight distributions of the top 20 000 compounds based on normalized and unnormalized vdW attractive energies obtained during primary database screening. Distribution for the entire database is also shown. (B) Molecular weight distributions of the top 500 compounds based on normalized and unnormalized total interaction energies obtained during secondary screening.

each compound was divided into nonoverlapping rigid segments connected by rotatable bonds. Segments with more than five heavy atoms were used as anchors, each of which was docked into the binding site in 250 orientations and minimized. The remainder of the molecule was built around the anchor in a stepwise fashion by adding other segments connected through rotatable bonds. At each step, the dihedral of the rotatable bond was sampled in increments of 10° and the lowest energy conformation was selected. During primary docking, each rotatable bond was minimized as it was created without reminimizing the other bonds. Pruning of the conformational orientations ensured conformational diversity and more favorable energies.[37,38] Energy scoring was performed with a distant-dependent dielectric, with a dielectric constant of 4, and using an all atom model. Once the whole molecule was built, then it was minimized. The conformation of each molecule with the most favorable interaction energy was selected and saved.

After the primary docking, compounds were chosen for the secondary screening based on their normalized vdW attractive interaction energy scores (see Results and Discussion). Compound selection based on the DOCK energy score favors compounds with higher molecular weight (MW) since their size contributes to the energy score. To minimize this size bias, an efficient procedure by which the DOCK energies are normalized by the number of heavy atoms N or by a power of N was applied.[36]

$$IE_{norm,vdW} = IE_{vdW}/N^{x}$$

Normalization of the vdW attractive energies was done with $x = 1$, 0.33, 0.5, and 0.67 and the MW distributions of the top 20 000 compounds in each category were analyzed, with $x = 1$ normalization used for the selection of compounds for secondary screening (see below).

The top 20 000 compounds obtained from the primary database search were screened in a more rigorous and computationally expensive docking procedure, referred to as secondary database screening. The procedure described for primary docking was followed with the additional step of minimizing all rotatable bonds simultaneously during the stepwise building of the molecule. The total interaction energies were then normalized via $N^{1/3}$ normalization, as performed above, and the top 500 compounds were selected and subjected to chemical diversity analysis.

Compound Selection Based on Chemical Diversity. Chemical similarity clustering of the top 500 compounds

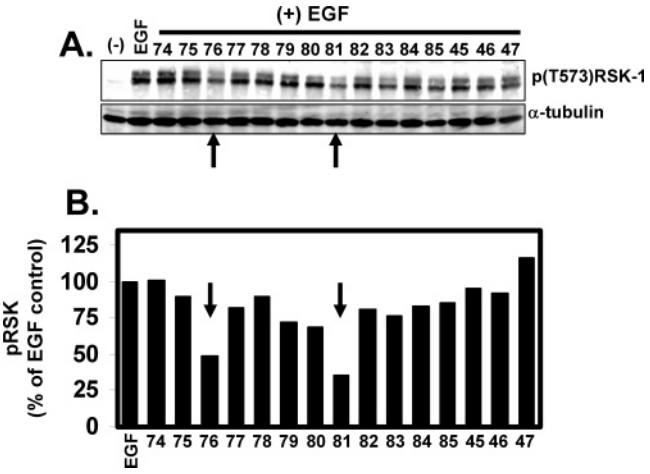

Figure 3. Effects of test compounds on Rsk-1 phosphorylation. HeLa cells were preincubated with 100 μM of test compounds and then stimulated for 5 min with EGF (50 ng/mL). Controls included untreated (−) and EGF-only treated cells. (A) Cell lysates were collected, separated by SDS−PAGE, and immunoblotted for phosphorylated Rsk-1 (pT573 RSK-1). The expression of α-tubulin is shown to demonstrate similar protein loading in each sample. (B) The relative amount of Rsk-1 phosphorylation in the immunoblot quantified by densitometry and normalized as a fraction of the α-tubulin levels. The pRsk-1 to tubulin ratio for the EGF only treatment was set at 100% and the pRsk-1 values for all other treatments were expressed as percentage of the EGF only control.

identified during secondary docking was performed to maximize the chemical diversity of the final compounds selected for biological assay. Clustering calculations were performed using the program MOE (Chemical Computing Group, Inc.). The Jarvis-Patrick algorithm, as implemented in MOE, was used to cluster the compounds using the MACC_BITS fingerprinting scheme and Tanimoto coefficient (TC). It first calculates the MACC_BITS fingerprints which encode the 2D structural features for each compound into linear bit strings of data. The pairwise similarity matrix between each compound was calculated based on the TC values.[39] TC is one of the metrics available that provides a similarity score by dividing the fraction of features common to both molecules by the total number of features. The similarity matrix is then converted into a second matrix in which each TC value is replaced by a 0 or 1 representing similarity values below and above the threshold value (S) provided by the user, respectively. The rows of the new matrix are treated as fingerprints and the 'TC' value between each is calculated. Molecules with values above the selected overlap threshold (T) are put in the same cluster. To select clusters of reasonable sizes (i.e. 1 to 20 compounds) an iterative procedure was followed in which the T value was gradually decreased by 10 and for each T value three S values (T-10, T-20, T-30) were calculated. Identified clusters of the appropriate size were removed from the list, stored for later analysis, and the remaining compounds were reclustered. This iterative approach produced a list in which the initial clusters had higher similarity than the later ones, which was taken into account in choosing the compounds for experimental testing.

Compounds for experimental assay were chosen from the individual clusters with emphasis on compounds with drug-like physical characteristics as defined by Lipinski et al.[40] Properties considered were the MW, number of hydrogen donors (NHD) and acceptors (NHA) and the logP values as calculated by MOE. However, exceptions were made when all compounds in a cluster had one or more physical characteristics beyond the range defined by Lipinski et al.[40] Compounds selected via CADD were purchased from ChemDiv (San Diego, CA) or ChemBridge (San Diego, CA) and dissolved in DMSO at a stock concentration of 25, 50, or 100 mM. The purity of the active compounds was verified by mass spectrometry and thin-layer chromatography using 90% chloroform and 10% methanol as the solvent. Cells were preincubated with the active compounds for 15−20 min prior to stimulation with EGF or PMA.

Cells and Reagents. HeLa (human cervical carcinoma), A549 (human lung carcinoma), HT1080 (human fibrosarcoma), or MDA-MB-468 (breast adenocarcinoma) cell lines were purchased from American Type Culture Collection (ATCC, Manassas, VA). The estrogen receptor negative breast cancer cells, SUM-159, were obtained from the University of Michigan Human Breast Cancer Cell SUM-Lines. All cell lines were cultured in a complete medium consisting of Dulbecco's modi-

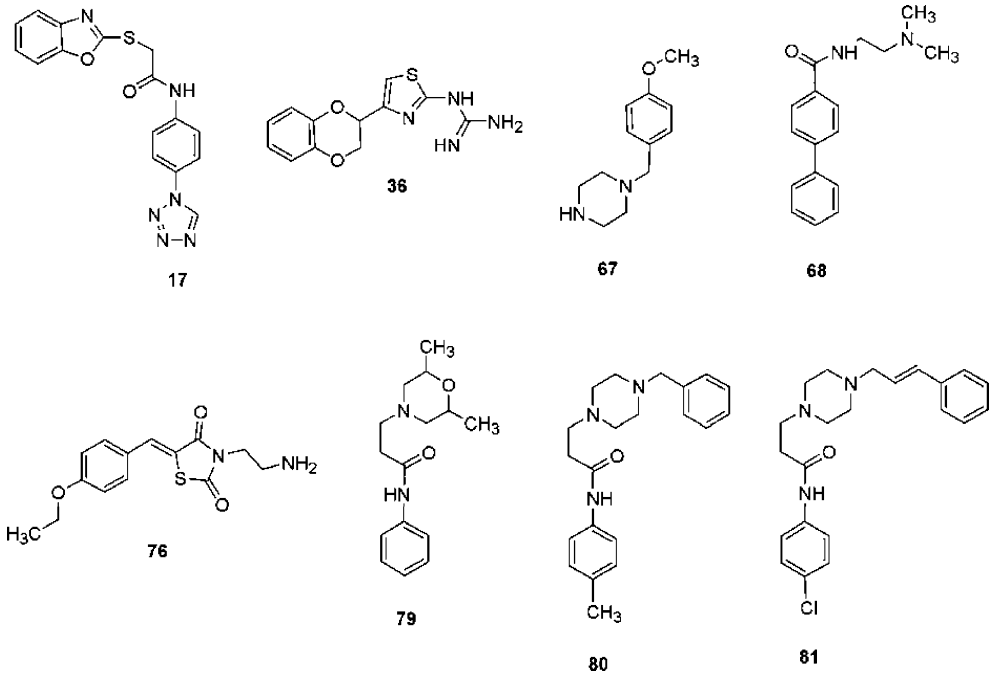

Figure 4. Chemical structures of compounds **17**, **36**, **67**, **76**, **79**, **80**, and **81** that showed greater than 25% inhibition of EGF-mediated phosphorylation of the ERK site (Thr573) on Rsk-1. Compound **68** was included as an example of a structure that did not inhibit Rsk-1 phosphorylation.

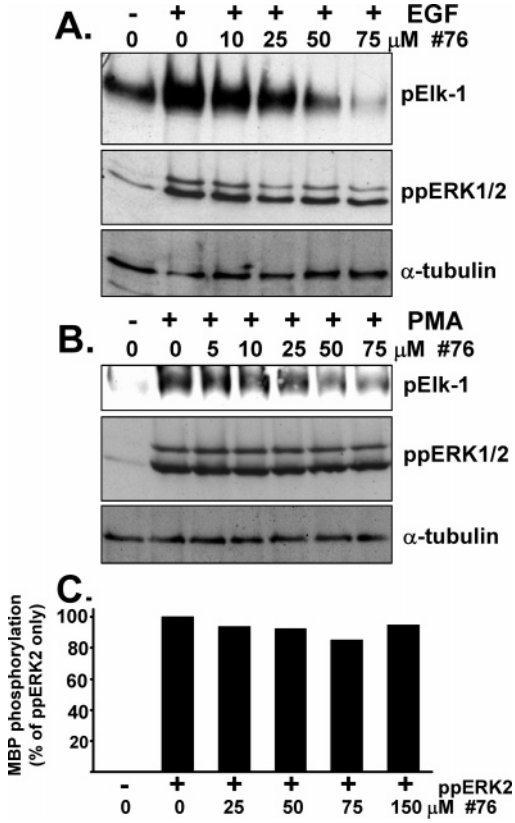

Figure 5. Effects of compound **76** on Elk-1 phosphorylation. Cells were pretreated with increasing concentrations of compound **76** and then stimulated with EGF in (A) or PMA in (B) for 5 min. The phosphorylation of Elk-1 on Ser383 (pElk-1) was measured by immunoblotting. The expression of dually phosphorylated ERK1/2 (ppERK1/2) and α-tubulin as a loading control are also shown. (C) Purified active ERK2 (ppERK2) was incubated with radiolabeled ATP and 2 μg myelin basic protein (MBP) as a nonspecific kinase substrate in the presence or absence of the indicated concentrations of compound **76**. Radiolabeled phosphate incorporation into MBP was quantified by phosphorimager analysis and graphed as a percentage of MBP phosphorylation in the presence of ppERK2 only.

fied Eagle medium (DMEM) supplemented with 10% fetal bovine serum (FBS) and antibiotics (penicillin, 100 U/ml; streptomycin, 100 μg/mL) (Invitrogen, Carlsbad, CA). epidermal growth factor (EGF), and phorbol 12-myristate 13-acetate (PMA) were purchased from Sigma (St. Louis, MO) and used at final concentrations of 50 ng/mL and 0.1 μM, respectively. Antibodies against phosphorylated Rsk-1 (pT573), Elk-1 (pS383), and ERK (pT183, pY185) were purchased from Cell Signaling Technologies (Woburn, MA), Santa Cruz Biotech. (Santa Cruz, CA), and Sigma, respectively. The α-tubulin antibody was purchased from Sigma.

ERK Substrate Phosphorylation and Immunoblotting. Control and treated cells were washed twice with cold phosphate buffered saline (PBS, pH 7.2; Invitrogen), and proteins were collected following cell lysis with 300 μL of cold tissue lysis buffer (20 mM Tris, pH 7.4, 137 mM NaCl, 2 mM EDTA, 1% Triton X-100, 0.1% SDS, 25 mM β-glycerophosphate, 2 mM sodium pyrophosphate, 10% glycerol, 1 mM sodium orthovanadate, 1 mM phenylmethylsulfonyl fluoride (PMSF), 1 mM benzamidine), allowed to incubate on ice for about 10 min, and then centrifuged at 20 000 (X g) to clarify the lysates of insoluble material. The lysates were then diluted with an equal volume of 2X SDS-sample buffer and the proteins were separated on SDS−PAGE for immunoblot analysis. Immunoblot analysis was done as previously described.[41−43]

In vitro ERK activity assays were done in a total volume of 20 μl by incubating purified active ERK2 (1 ng, New England Biolabs; Beverly, MA) with 2 μg myelin basic protein (MBP, Sigma) in kinase buffer (50 mM Hepes, pH 7.4, 10 mM $MgCl_2$, and 2 mM DTT) plus 10 μCi ^{32}P ATP at 30°C for 30 min. Test compounds were added at a final concentration of 0−150 μM. Samples were analyzed by SDS−PAGE and radiolabeled phosphate incorporation into MBP was quantified by phosphorimaging.

Colony Formation Assay. Two methods were used to determine cell proliferation and survival based on colony formation. First, cells were grown to 70−80% confluence and then treated for 16 h in the absence (DMSO only) or presence of active compounds. The next day cells were trypsinized, replated (1000−2000 cells per 10 cm culture dish) in regular media, and allowed to grow for 8−14 days. Cells were then fixed for 10 min in 4% paraformaldehyde and stained with 0.2% crystal violet (in 20% methanol) for 1−2 min. Cells were washed several times with distilled water and colonies formed (at least 40 cells) were counted. In the second method, growing cells were trypsinized and replated (500−1000 cells per 35 or 60 mm well, respectively) in the presence or absence of various concentrations of the test compounds. Following incubation for 8−14 days, cells were fixed, stained with crystal violet, and counted as described above.

Fluorescence Spectroscopy. a. Protein Purification. ERK2 was purified as described previously[44] with some modifications. Briefly, $(His)_6$-tagged ERK2 was bacterially expressed and the cells harvested in BugBuster protein extraction reagent (EMD Biosciences, San Diego, CA). Clarified lysates were loaded onto a Talon Co^{2+}-IMAC affinity chromatography resin column (BD Biosciences, San Jose, CA), and the bound protein eluted using increasing concentrations of imidazole. SDS−PAGE electrophoresis and Coomassie blue staining were used to identify the eluted fractions containing the ERK2 protein. The ERK2 protein concentration was determined using Bradford Reagent (Sigma).

b. Fluorescence Titrations. Fluorescence spectra were recorded with a Luminescence Spectrometer LS50 (Perkin-Elmer, Boston, MA). For all experiments, ERK2 protein was diluted into 20 mM Tris-HCl, pH 7.5. Titrations were performed by increasing the test compound concentration while maintaining the ERK2 protein concentration at 3 mM. The excitation wavelength was 295 nm and fluorescence was monitored from 300 to 500 nm. All reported fluorescence intensities are relative values and are not corrected for wavelength variations in detector response. Dissociation constants, K_D, were determined using reciprocal plots, $1/\nu$ vs 1/[I], where ν represents the percent occupied sites calculated assuming fluorescence quenching to be directly proportion to the percentage of occupied binding sites, [I] represents the concentration of the inhibitor compound and the slope of the curve equals the K_D.[45] For inhibitor **36**, the maximal quenching was assumed to be equivalent to that obtained with **76** and with both **36** and **76** the data point associated with the lowest concentration of inhibitor (0.1 μM) was excluded from the linear regression analysis.

Results and Discussion

ERK2 Structure and Location of Substrate Docking Domains. The ERK2 structure (Figure 1A) is bilobal in nature typical of many kinases where the amino and carboxyl lobes are separated by a hinge region.[27] Upon phosphorylation of Thr183 and Tyr185 a conformational change brings the N-terminal lobe containing the ATP binding site in proximity to the C-terminal lobe to allow phosphate transfer onto substrate proteins. Previous studies suggest that the substrate proteins interactions with ERK2 were determined by common docking (CD) and ED domain regions in the C-terminus that interact with substrate binding motifs.[14,34] Accordingly, we selected the CD and ED domain

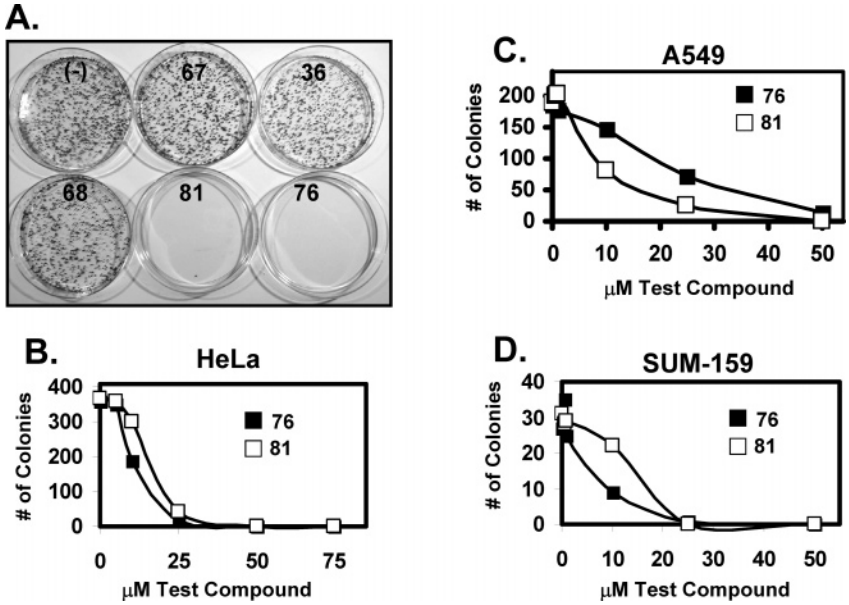

Figure 6. Inhibition of cell proliferation with test compounds. HeLa, A549, or SUM-159 cells were plated at a low density in the absence or presence of putative ERK docking domain inhibitors (50 μM) and cell colonies were analyzed after 10 days. (A) HeLa cell colonies stained with crystal violet following incubation with DMSO (control) or the test compounds (**67**, **36**, **68**, **81**, or **76**). The number of cell colonies that formed after incubation with varying concentrations of test compounds **76** (closed squares) or **81** (open squares) were graphed for (B) HeLa, (**C**) A549, or (**D**) SUM-159 cells.

region for the identification of putative binding sites. Inhibitors that bind to such sites will have the potential for blocking ERK2-substrate protein interactions, with the inhibition potentially being specific for certain substrate proteins.

Using the program SPHGEN, potential binding sites on the ERK2 protein were identified and the sites in the region of the CD and ED domains were analyzed in detail. This led to the identification of a putative cleft between the CD and ED domains, which reside on the opposite side of the activation loop (Figure 1A) and are involved in ERK substrate interactions. The CD domain includes Asp316 and Asp319 in the C-terminus[16] and the ED domain includes residues Thr157 and Thr158. Figure 1B shows a space-filling model of the protein illustrating the cleft between CD and ED. This cleft was used as the target binding site for the CADD screening.

Primary Database Screening. Compound selection from the primary database screen was based on the vdW attractive energy, as previously performed.[26] Use of this term selected compounds that have favorable steric interactions with the protein and avoids the selection of compounds whose interaction with the protein are dominated by one or two electrostatic interactions. Use of the vdW attractive term for scoring does not exclude the selection of compounds for which favorable electrostatic interactions with the protein occur as the total energy (i.e. electrostatic and vdW terms) was used for the actual docking process (i.e. posing). Use of the vdW attractive energy without any normalization yielded an average MW for the top scoring 20 000 compounds of 457 Da (Figure 2A). This means that approximately half of those compounds were above a MW of 500 Da. As drug-like compounds typically have MWs below 500 Da[40] and lead compounds, the target of the present study, have even lower MWs,[46] compounds with lower MWs were selected via the previously developed normalization procedure.[36] Using N, $N^{2/3}$, $N^{1/2}$, and $N^{1/3}$ normalization the average MWs were 248, 317, 368, and 410 Da, respectively. Figure 2A shows how larger powers of N shift the MW distribution of the selected compounds toward lower MW values. To choose the normalization procedure for compound selection it should be noted that the MW probability distribution of the entire database screened in the present study was centered at 364 Da, while the average of the World Index Database is at 359 Da.[36] Thus, N normalization was chosen since lead compounds of lower MW are desired. The smaller MW of the lead compounds will allow the addition of functional groups during future lead optimization efforts.

It should be noted that significant overlap of compounds occurred for the different normalization schemes. Of the 20 000 compounds selected via N normalization, 11355 compounds were common in the $N^{2/3}$set, 6540 in the $N^{1/2}$set, 3292 in the $N^{1/3}$ set and 815 were in the set of nonnormalized compounds. Thus, it may be assumed that compounds with highly favorable interaction orientations with the protein binding site were not being excluded by the normalization procedure.

Secondary Database Screening. Secondary screening of the 20 000 compounds selected from the primary screen involved a more exhaustive and computationally demanding conformational search of the docked molecules. As compounds with good steric fit were selected from the primary screen, electrostatic as well as vdW interaction energies were used for the selection of compounds from the secondary screen. Thus, the total interaction energies were normalized and the MW distributions of the top 500 compounds in each set using different powers of N was determined (Figure 2B). For the top 500 compounds selected via the N, $N^{2/3}$, $N^{1/2}$, and $N^{1/3}$ normalization, the average distributions were 210, 226, 238, and 267 Da, respectively (Figure 2B). The average for the top 500 compounds without normalizing the energies was 321 Da (Figure 2B). The top 500 scoring compounds in the set obtained after $N^{1/3}$ normalization was chosen to avoid molecules which were

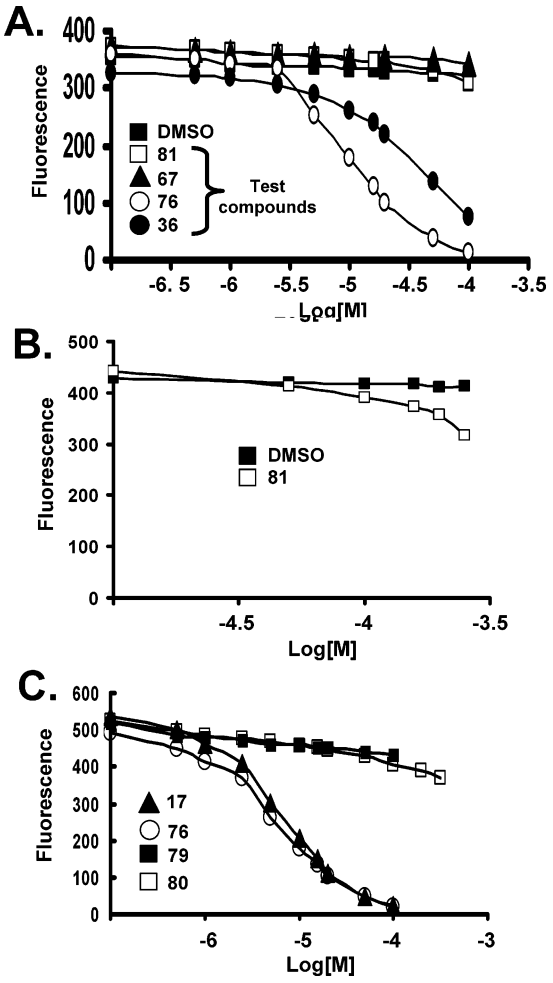

Figure 7. Effect of test compounds on ERK2 fluorescence. (A) Fluorescence titration of ERK2 was done with selected compounds. The fluorescence (F) is plotted against the log concentration in moles/liter (Log [M]) for each compound is shown. Data are included for compounds **81** (open squares), **67** (closed triangles), **76** (open circles), and **36** (closed circles). (B) Fluorescence quenching of ERK2 with higher doses of test compound **81**. (C) Fluorescence titration of ERK2 with compounds **17** (closed triangles), **76** (open circles), **79** (closed triangles), or **80** (open squares).

too small and lacking adequate structure diversity for lead or drug-like candidates.

Final Compound Selection. The final list of compounds to be submitted for experimental testing should be chemically diverse to increase the probability of identifying unique leads.[26] To facilitate selection of diverse compounds, a clustering algorithm that distributes the compounds into groups (clusters) of structurally similar compounds with compounds across clusters being dissimilar was applied. One or more compounds were selected from each cluster. This selection process was based on Lipinski's Rule of 5; MW was less than 500 Da and the number of hydrogen bond donors, the number of hydrogen bond acceptors and logP values were each less than 5 although exceptions were made for clusters that did not contain members fulfilling these criteria. These properties increase the likelihood that the compound will have good ADME properties according to Lipinski's rules.[40] A total of 86 compounds were selected from which 80 were obtained from commercial sources and subjected to biological assays.

Compounds Effects on ERK Substrate Phosphorylation. All obtained compounds were subjected to assays of ERK specific phosphorylation of Rsk-1 and Elk-1 as examined by immunoblot analysis using phosphorylation specific antibodies. HeLa cells were pretreated with the test compounds at a concentration of 100 μM and then stimulated with EGF for 5 min to activate the ERK pathway. Cell lysates were collected and immunoblotted for ERK-mediated phosphorylation of Rsk-1 on Thr573. As shown, EGF treatment alone caused a robust increase in Thr573 phosphorylation on Rsk-1 in the absence of test compounds (Figure 3A). A typical immunoblot for Rsk-1 phosphorylation in the presence of 15 test compounds is shown in Figure 3A. The presence of test compounds had varying inhibitory effects on ERK-mediated Rsk-1 phosphorylation (Figure 3A). In these samples, densitometry quantification of the immunoblots showed that two compounds caused greater than 50% inhibition of Rsk-1 phosphorylation (Figure 3B). Four additional compounds (**17**, **36**, **79**, and **80**) inhibited ERK-mediated Rsk-1 phosphorylation by 20−25% out of the 80 compounds tested (data not shown). The structures of the active compounds are shown in Figure 4.

The ERK-specific phosphorylation of the transcription factor Elk-1 on Ser383 was also tested with the compounds that showed the highest inhibition of Rsk-1 phosphorylation in Figure 3A (i.e. compound **76**). As shown, increasing doses of **76** inhibited ERK-mediated Elk-1 phosphorylation in response to EGF or PMA stimulation (Figure 5A and B). As a protein loading control, the expression of α-tubulin was unchanged (Figure 5A and B). Importantly, ERK1/2 phosphorylation on its activating sites was largely unaffected by the test compound (Figure 5A and B). To further confirm that **76** does not affect ERK catalytic activity, an in vitro cell free kinase assay, which contained purified active ERK2 plus the nonspecific substrate myelin basic protein (MBP), was performed with and without various concentrations of compound **76**. As shown, concentrations of **76** up to 150 μM had little effect on the ability for ERK2 to phosphorylate MBP (Figure 5C). This finding supports the specificity of this test compound for inhibiting ERK phosphorylation of downstream substrates while having little effect on ERK protein phosphorylation by its upstream activator MEK1/2.

Effects of Active Compounds on Cell Proliferation. The effects of the active compounds on cell proliferation and survival were tested using a colony formation assay. A screen of five test compounds showed that two compounds (**76** and **81**) completely inhibited cell proliferation as evident by decreased number of cell colonies (Figure 6A). Compound **36** showed subtle inhibition of colony formation (Figure 6A), which was confirmed in additional experiments (data not shown). Compounds **67** and **68** had little effect on cell proliferation and were not tested further. Dose response assays demonstrated that compounds **76** and **81** similarly inhibited HeLa cell colony formation with an IC_{50} of approximately 15−20 μM (Figure 6B). In A549 lung carcinoma cells the IC_{50} for compounds **76** and **81** was approximately 25 and 15 μM, respectively (Figure 6C). Moreover, inhibition of cell proliferation following incubation with **76** and **81** was observed in the SUM-159

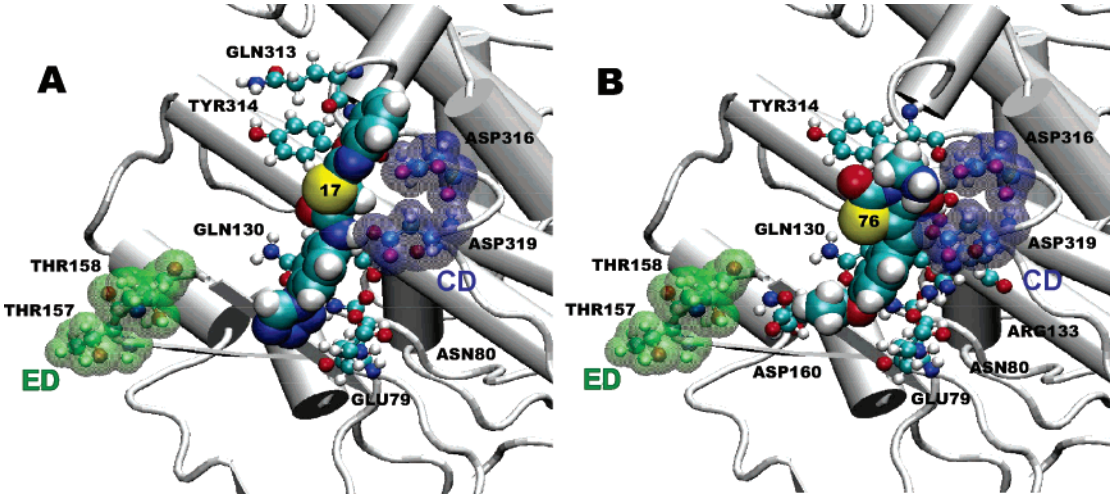

Figure 8. Predicted binding of active compounds to ERK2. The binding mode of **17** (A) or **76** (B) is shown. The ERK2 structure is shown in gray. The space-filling model of the docked compounds is predicted to form contacts with several amino acids within the groove between Asp316 and Asp319 of the CD domain (blue spheres) and Thr157 and Thr158 of the ED domain (green spheres). Sulfur, oxygen, or nitrogen atoms on the active compounds are indicated as yellow, red, or blue spheres, respectively.

estrogen-receptor negative breast cancer cell line (Figure 6D) and HT1080 fibrosarcoma cells (data not shown). Last, **17**, **79**, and **80** also inhibited HeLa, A549, HT1080, and MDA-MB-468 cell proliferation with IC_{50} values similar to **76** and **81** (data not shown). Thus, several test compounds that show maximal inhibition of ERK substrates were also effective inhibitors of proliferation in cultured cancer cell lines.

Fluorescence Titrations. We next determined whether the active compounds directly interact with ERK2 using fluorescence quenching taking advantage of the three tryptophans in the protein. Of the two compounds shown to be the most active in all biological assays, **76** and **81**, **76** shows strong quenching of fluorescence while quenching only occurs to a small extent at the higher concentrations with **81** (Figure 7A and B). Compound **36** also showed significant quenching (Figure 7A). Interestingly, **36**, which also had little effect on ERK-mediated Rsk-1 phosphorylation (data not shown) but caused a subtle inhibition of colony formation (Figure 6A), showed significant binding with ERK2 (Figure 7A). Thus, this compound may be useful for future analysis of ERK function and substrate phosphorylation. In addition, **67** was included as a negative control, as it showed inhibition of Rsk-1 phosphorylation (data not shown) but had little effect on colony formation (Figure 6A). However, this compound did not show quenching at the concentrations tested (Figure 7A).

Based on reciprocal plots K_D values of 5 and 16 μM were calculated for **76** and **36**, respectively, with y-intercepts of 1.8 and 1.1, respectively, indicating a single binding site on the protein. Thus, the fluorescence quenching experiments indicate that **76** is binding directly to ERK2, thereby leading to its biological activity. Importantly, the K_D for compound **76**, as determined from the fluorescence quenching, is similar to the approximate IC_{50} determined based on colony formation (Figure 6). Compound **17**, which also inhibited colony formation, had a similar K_D as **76** (Figure 7C). However, **79**, **80**, and **81**, which are similarly efficacious in the colony formation assay, bind poorly to ERK2 based on fluorescence quenching, although some binding is indicated by the quenching occurring at higher concentrations (Figure 7B and C). These findings suggest that the effects of compounds **79**, **80**, and **81** on ERK phosphorylation and cell proliferation may not be via ERK-specific interactions.

Predicted Structures of Ligand-ERK2 Complexes. As the experimental fluorescence results confirm that compounds **17** and **76** bind to directly ERK2, it is of interest to understand the nature of the interactions between those compounds and ERK2. A detailed atomic picture of the predicted binding modes for these compounds based on the Method 2 screen is presented in Figure 8. Based on these predicted binding conformations, the compounds fit nicely into the groove that is located between the ED and CD sites. With both compounds, binding is predicted to occur adjacent to the CD site which places the compounds approximately 5−7 Å away from the threonine residues of the ED site, which forms a small protrusion on the protein surface.

The groove into which the compounds bind is polar containing several charged amino acids that are involved in multiple favorable interactions with the compounds. ERK2 residues with atoms within 3 Å of the compounds were Glu79, Asn80, Gln130, Arg133, Tyr314, Gln313, and the two aspartates from the CD site, Asp316 and Asp319. Several hydrogen bonds are observed between the aspartates and **17** and **76** (Figure 8A and B). Arg133 is located above the aromatic rings in **76** and **17** potentially forming a cation-π bond. Tyr314 makes a CH···O interaction through its backbone oxygen with **76**. In addition, if the protein structure was allowed to relax around the bound compound, it is likely that more inhibitor-ERK2 interactions would be identified. Thus, based on the predicted binding interactions, a number of inhibitor-protein interactions may contribute to both the binding affinity and the selectivity for the ERK2 protein. Additional studies beyond the scope of the present work, including X-ray crystallography or NMR spectroscopy, are required to verify the present predicted binding orientations.

Conclusions

Inhibitors of ERK protein docking domains represent a unique approach to selectively block substrate interac-

tions. By targeting unique regions on ERK, we predict that increased selectivity of these compounds will be achieved compared to typical kinase inhibitors that act as competitive inhibitors of ATP. The ERK proteins may target dozens of different substrates in vivo. Selective inhibition of substrates involved in unregulated cell proliferation may be achieved by targeting ERK docking domains. Thus, we propose that the CADD approach will allow the identification of compounds that disrupt ERK interactions with substrates involved in pathobiological conditions, such as cancer cell proliferation, while preserving ERK interactions with substrates needed for normal metabolic processes and cell maintenance. Such an approach of selective inhibition of ERK substrates may also reduce toxicity to normal cells, which is observed with many of the current chemotherapies. The CADD described in the current studies may also be applied to target docking domains of other MAP kinases, such as p38, to develop novel immunosuppressant agents.

Several of the 80 computationally selected compounds showed some inhibitory effects on ERK induced phosphorylation of Rsk-1 (Figure 3). Additional biological screening showed that five compounds (**17**, **76**, **79**, **80**, and **81**) were effective inhibitors of cell proliferation in the colony formation assay. Of these compounds, **17** and **76** were shown to directly interact with the ERK2 protein using fluorescence titrations. Thus, CADD in combination with experimental assays can identify compounds whose biological actions are ERK-dependent. However, careful experimental analysis of the compounds is necessary to ensure that the compounds do indeed function via an ERK-dependent fashion. In the case of compounds **79**, **80**, and **81**, biological activity was seen in the low micromolar range while fluorescence quenching experiments indicate ERK2 binding to occur an order of magnitude more poorly, suggesting the possibility of an ERK-independent mechanism for these inhibitors. Future studies will look at the mode of activity of these compounds as well as expand the CADD screen to identify additional molecules that will act as lead compounds for the development of novel ERK inhibitors that can be used for experimental and clinical purposes.

Acknowledgment. This work was supported by grants (CA105299-01 to P.S., CA95200-01 to A.D.M., and CA095200-03S1 to A.M.) from the National Institutes of Health and the University of Maryland, School of Pharmacy Computer-Aided Drug Design Center. We thank Dr. Angela Wilks and Ila Goldstein for assistance with the fluorescence titrations, Dr. Julie Ray for mass spectrometry analysis, and Dr. Andrew Coop for thin-layer chromatography analysis.

References

(1) Pearson, G.; Robinson, F.; Beers Gibson, T.; Xu, B. E.; Karandikar, M.; Berman, K.; Cobb, M. H. Mitogen-activated protein (MAP) kinase pathways: regulation and physiological functions. *Endocr. Rev.* **2001**, *22*, 153−183.

(2) Kyriakis, J. M.; Avruch, J. Protein kinase cascades activated by stress and inflammatory cytokines. *Bioessays* **1996**, *18*, 567−577.

(3) Reuter, C. W.; Morgan, M. A.; Bergmann, L. Targeting the Ras signaling pathway: a rational, mechanism-based treatment for hematologic malignancies? *Blood* **2000**, *96*, 1655−1669.

(4) Duesbery, N. S.; Webb, C. P.; Vande Woude, G. F. MEK wars, a new front in the battle against cancer. *Nat. Med.* **1999**, *5*, 736−737.

(5) Shapiro, P. Ras-MAP kinase signaling pathways and control of cell proliferation: relevance to cancer therapy. *Crit. Rev. Clin. Lab. Sci.* **2002**, *39*, 285−330.

(6) Cohen, P. The development and therapeutic potential of protein kinase inhibitors. *Curr. Opin. Chem. Biol.* **1999**, *3*, 459−465.

(7) Lewis, T. S., Shapiro, P. S., Ahn, N. G. Signal tranduction through MAP Kinase Cascades. *Adv. Cancer Res.* **1998**, *74*, 49−139.

(8) Zhang, J.; Zhang, F.; Ebert, D.; Cobb, M. H.; Goldsmith, E. J. Activity of the MAP kinase ERK2 is controlled by a flexible surface loop. *Structure* **1995**, *3*, 299−307.

(9) Bos, J. L. ras oncogenes in human cancer: a review. *Cancer Res.* **1989**, *49*, 4682−4689.

(10) Brose, M. S.; Volpe, P.; Feldman, M.; Kumar, M.; Rishi, I.; Gerrero, R.; Einhorn, E.; Herlyn, M.; Minna, J.; Nicholson, A.; Roth, J. A.; Albelda, S. M.; Davies, H.; Cox, C.; Brignell, G.; Stephens, P.; Futreal, P. A.; Wooster, R.; Stratton, M. R.; Weber, B. L. BRAF and RAS mutations in human lung cancer and melanoma. *Cancer Res.* **2002**, *62*, 6997−7000.

(11) Songyang, Z.; Lu, K. P.; Kwon, Y. T.; Tsai, L. H.; Filhol, O.; Cochet, C.; Brickey, D. A.; Soderling, T. R.; Bartleson, C.; Graves, D. J.; DeMaggio, A. J.; Hoekstra, M. F.; Blenis, J.; Hunter, T.; Cantley, L. C. A structural basis for substrate specificities of protein Ser/Thr kinases: primary sequence preference of casein kinases I and II, NIMA, phosphorylase kinase, calmodulin-dependent kinase II, CDK5, and Erk1. *Mol. Cell Biol.* **1996**, *16*, 6486-6493.

(12) Zuniga, A.; Torres, J.; Ubeda, J.; Pulido, R. Interaction of mitogen-activated protein kinases with the kinase interaction motif of the tyrosine phosphatase PTP−SL provides substrate specificity and retains ERK2 in the cytoplasm. *J. Biol. Chem.* **1999**, *274*, 21900−21907.

(13) Fantz, D. A.; Jacobs, D.; Glossip, D.; Kornfeld, K. Docking sites on substrate proteins direct extracellular signal-regulated kinase to phosphorylate specific residues. *J. Biol. Chem.* **2001**, *276*, 27256−27265.

(14) Zhang, J.; Zhou, B.; Zheng, C. F.; Zhang, Z. Y. A bipartite mechanism for ERK2 recognition by its cognate regulators and substrates. *J. Biol. Chem.* **2003**, *278*, 29901−29912.

(15) Nichols, A.; Camps, M.; Gillieron, C.; Chabert, C.; Brunet, A.; Wilsbacher, J.; Cobb, M.; Pouyssegur, J.; Shaw, J. P.; Arkinstall, S. Substrate recognition domains within extracellular signal-regulated kinase mediate binding and catalytic activation of mitogen-activated protein kinase phosphatase-3. *J. Biol. Chem.* **2000**, *275*, 24613−24621.

(16) Tanoue, T.; Adachi, M.; Moriguchi, T.; Nishida, E. A conserved docking motif in MAP kinases common to substrates, activators and regulators. *Nat. Cell Biol.* **2000**, *2*, 110−116.

(17) Bollag, G.; Freeman, S.; Lyons, J. F.; Post, L. E. Raf pathway inhibitors in oncology. *Curr. Opin. Investig. Drugs* **2003**, *4*, 1436−1441.

(18) Boldt, S.; Kolch, W. Targeting MAPK signaling: Prometheus' fire or Pandora's box? *Curr. Pharm. Des.* **2004**, *10*, 1885−1905.

(19) Sebolt-Leopold, J. S. MEK inhibitors: a therapeutic approach to targeting the Ras-MAP kinase pathway in tumors. *Curr. Pharm. Des.* **2004**, *10*, 1907−1914.

(20) Allen, L. F.; Sebolt-Leopold, J.; Meyer, M. B. CI-1040 (PD184352), a targeted signal transduction inhibitor of MEK (MAPKK). *Semin. Oncol.* **2003**, *30*, 105−116.

(21) Bain, J.; McLauchlan, H.; Elliott, M.; Cohen, P. The specificities of protein kinase inhibitors: an update. *Biochem. J.* **2003**, *371*, 199−204.

(22) Gohlke, H.; Klebe, G. Approaches to the description and prediction of the binding affinity of small-molecule ligands to macromolecular receptors. *Angew. Chem., Int. Ed.* **2002**, *41*, 2644−2676.

(23) Markowitz, J.; Chen, I.; Gitti, R.; Baldisseri, D. M.; Pan, Y.; Udan, R.; Carrier, F.; MacKerell, A. D., Jr.; Weber, D. J. Identification and characterization of small molecule inhibitors of the calcium-dependent S100B−p53 tumor suppressor interaction. *J. Med. Chem.* **2004**, *47*, 5085−5093.

(24) Loughney, D. A., Murray, W. V., and Jolliffe, L. K. Application of Virtual Screening Tools to a Protein−Protein Interaction: Database Mining Studies on the Growth Hormone Receptor. *Med. Chem. Res.* **1999**, *9*, 579−591.

(25) Zeng, J.; Nheu, T.; Zorzet, A.; Catimel, B.; Nice, E.; Maruta, H.; Burgess, A. W.; Treutlein, H. R. Design of inhibitors of Ras- -Raf interaction using a computational combinatorial algorithm. *Protein Eng.* **2001**, *14*, 39−45.

(26) Huang, N.; Nagarsekar, A.; Xia, G.; Hayashi, J.; MacKerell, A. D., Jr. Identification of nonphosphate-containing small molecular weight inhibitors of the tyrosine kinase p56 Lck SH2 domain via in silico screening against the pY + 3 binding site. *J. Med. Chem.* **2004**, *47*, 3502−3511.

(27) Zhang, F.; Strand, A.; Robbins, D.; Cobb, M. H.; Goldsmith, E. J. Atomic structure of the MAP kinase ERK2 at 2.3 A resolution. *Nature* **1994**, *367*, 704−711.

(28) Canagarajah, B. J.; Khokhlatchev, A.; Cobb, M. H.; Goldsmith, E. J. Activation mechanism of the MAP kinase ERK2 by dual phosphorylation. *Cell* **1997**, *90*, 859−869.
(29) Bernstein, F. C.; Koetzle, T. F.; Williams, G. J.; Meyer, E. F., Jr.; Brice, M. D.; Rodgers, J. R.; Kennard, O.; Shimanouchi, T.; Tasumi, M. The Protein Data Bank. A computer-based archival file for macromolecular structures. *Eur. J. Biochem.* **1977**, *80*, 319−324.
(30) Kuntz, I. D.; Blaney, J. M.; Oatley, S. J.; Langridge, R.; Ferrin, T. E. A geometric approach to macromolecule-ligand interactions. *J. Mol. Biol.* **1982**, *161*, 269−288.
(31) Kuntz, I. D. Structure-based strategies for drug design and discovery. *Science* **1992**, *257*, 1078−1082.
(32) Connolly, M. L. Solvent-accessible surfaces of proteins and nucleic acids. *Science* **1983**, *221*, 709−713.
(33) Ferrin, T. E.; Huang, C. C.; Jarvis, L. E.; Langridge, R. The MIDAS display system. *J. Mol. Graphics* **1988**, *6*, 13−27.
(34) Tanoue, T.; Maeda, R.; Adachi, M.; Nishida, E. Identification of a docking groove on ERK and p38 MAP kinases that regulates the specificity of docking interactions. *EMBO J.* **2001**, *20*, 466−479.
(35) Goodford, P. J. A computational procedure for determining energetically favorable binding sites on biologically important macromolecules. *J. Med. Chem.* **1984**, *28*, 849−857.
(36) Pan, Y.; Huang, N.; Cho, S.; MacKerell, A. D., Jr. Consideration of molecular weight during compound selection in virtual target-based database screening. *J. Chem. Inf. Comput. Sci.* **2003**, *43*, 267−272.
(37) Leach, A. R.; Kuntz, I. D. Conformational analysis of flexible ligands in macromolecular receptor sites. *J. Comput. Chem.* **1992**, *13*, 730−748.
(38) Ewing, T. J. A.; Kuntz, I. D. Critical evaluation of search algorithms used in automated molecular docking. *J. Comput. Chem.* **1997**, *18*, 1175−1189.
(39) Butina, D. Unsupervised database clustering on daylight's fingerprint and Tanimoto similarity: A fast and automated way to cluster small and large data sets. *J. Chem. Inf. Comput. Sci.* **1999**, *39*, 747−750.
(40) Lipinski, C. A.; Lombardo, F.; Dominy, B. W.; Feeney, P. J. Experimental and computational approaches to estimate solubility and permeability in drug discovery and development settings. *Adv. Drug Delivery Rev.* **2001**, *46*, 3−26.
(41) Cha, H.; Lee, E. K.; Shapiro, P. Identification of a C-terminal Region That Regulates Mitogen-activated Protein Kinase Kinase-1 Cytoplasmic Localization and ERK Activation. *J. Biol. Chem.* **2001**, *276*, 48494−48501.
(42) Dangi, S.; Cha, H.; Shapiro, P. Requirement for phosphatidylinositol-3 kinase activity during progression through S-phase and entry into mitosis. *Cell Signal* **2003**, *15*, 667−675.
(43) Cha, H.; Hancock, C.; Dangi, S.; Maiguel, D.; Carrier, F.; Shapiro. P. Phosphorylation regulates nucleophosmin targeting to the centrosome during mitosis as detected by cross reactive phosphorylation specific MKK1/2 antibodies. *Biochem. J.* **2004**, *378*, 857−865.
(44) Shapiro, P. S.; Whalen, A. M.; Tolwinski, N. S.; Wilsbacher, J.; Froelich-Ammon, S. J.; Garcia, M.; Osheroff, N.; Ahn, N. G. Extracellular signal-regulated kinase activates topoisomerase IIalpha through a mechanism independent of phosphorylation. *Mol. Cell Biol.* **1999**, *19*, 3551−3560.
(45) Marshall, G. *Biophysical Chemistry: Principles, Techniques, and Applications*; John Wiley & Sons: New York, 1978.
(46) Oprea, T. I.; Davis, A. M.; Teague, S. J.; Leeson, P. D. Is there a difference between leads and drugs? A historical perspective. *J. Chem. Inf. Comput. Sci.* **2001**, *41*, 1308−1315.

JM0501174